

# Revolute joints with clearance and impacts: image analysis of high speed camera recordings

Alessandro Tasora, Edzeario Prati, Marco Silvestri  
*Università degli Studi di Parma, Dipartimento di Ingegneria Industriale  
Parco Area delle Scienze, 43100 Parma, Italy*

*Keywords:* revolute joints, clearance, high speed film, camera, image analysis.

**SUMMARY.** This proposal describes a device which allows the high-speed film recording of oscillatory phenomena in a moving revolute joint affected by clearance. The revolute joint is mounted between the rocker and the rod of a four-bar linkage, thus the center of the bushing follows a fast arched trajectory. Even if the videocamera is mounted on a steady and fixed position, a continuous close-up film of the revolute joint is possible thanks to an optical system based on two mirrors which acts like a periscope.

## 1 INTRODUCTION

Clearance in revolute pairs of articulated mechanisms are major sources of noise, premature wear and low precision [P. Flores, 2006].

A custom four bar linkage has been built for experimental investigations about the effect of clearances: previous researches of ours showed how this test bed provided a validation of our numerical method for simulating clearances [A. Tasora, 2003], either in terms of accelerations [A. Tasora, 2004], wear [A. Tasora, 2005] and displacements [A. Tasora, 2006].

Hence, this paper complements these analyses by means of video recordings of the motion of the shaft respect to the bushing, using a video camera which is capable of image acquisition at high speeds, up to 1000 fps. Within this experimental context the revolute joint with clearance connects the rod and the rocker, therefore describes a fast arched trajectory respect to the ground.

Since it is not practical to move the camera together with the rocker, we built a lightweight device made of two mirrors, both connected to the rocker, as shown in Fig.1.

Given a precise positioning of these mirrors and a specific alignment between lenses and the oscillating periscope, the picture of the moving revolute joint will remain always centered in the field of view of the camera, allowing a continuous close-up recording of impacts and vibrations within the clearance.

We performed tests at different speeds and with different clearance values, obtaining video sequences whose resolution is detailed enough to show the position of the point of contact with clearances of moderate value. Also, conditions affected by loss of contact and subsequent impacts, which are important phenomena in this context [P. Flores, 2004], can be easily detected.

Video sequences can be subject to automated image analysis, using artificial vision tools like convolution filters, masking, feature recognition and extraction, in order to obtain graphs which show the position of the point of contact as a function of the time.

Figure 2 shows the references used in the revolute joint with clearance. Thanks to the abovementioned automatic image analysis, it is possible to compute the phase  $\varphi$  of the contact point as well as, with lower precision, the displacements  $x$ ,  $y$  and  $\rho$ .

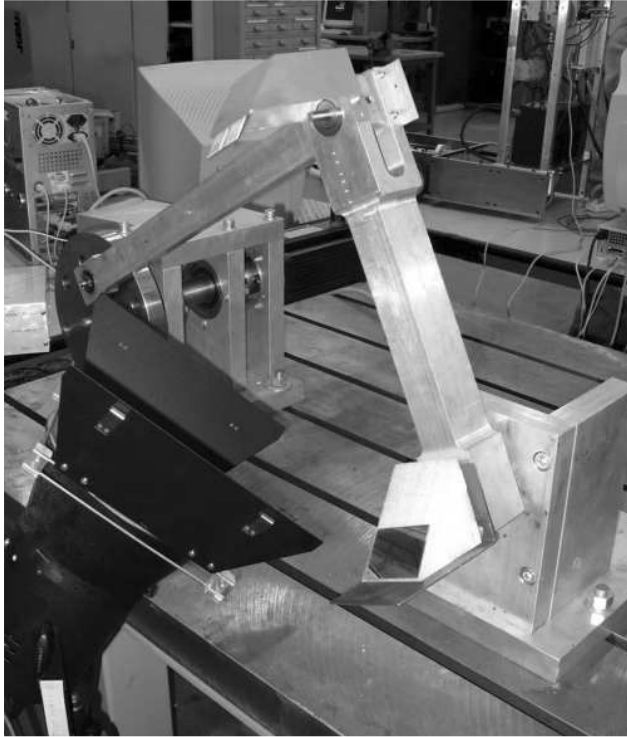


Figure 1: The four bar linkage, with the mirrors mounted on the rocker. Note the lamp on the left, pointing toward the revolute joint.

## 2 SETUP OF THE OPTICAL DEVICE

Close-up films of moving parts could be performed using flexible bundles of optical fibers, such as in fiberscopes used for endoscopic surgery. However this approach might be limited in terms of accelerations, toughness and affordability. For this reason we propose a device which acts like a periscope: since it is essentially based on two mirrors, it is cheap, simply to build and can be easily adapted to many types of videocameras and articulated devices.

The scheme of the system is sketched in Fig.3. Two mirrors are stiffly connected to the swinging rocker: the former is mounted with its center on the  $KC$  axis of the rotation of the rocker about the truss, and the latter is mounted with its center on the axis of the revolute joint between the rocker and the rod. Both mirrors are parallel and tilted  $45^\circ$  about their horizontal axes; also they are aligned along a line parallel to the rocker. This configuration is similar to a periscope which rotates together with the rocker.

If the configuration of Fig.3 is satisfied, the image of the joint in  $A$  will be reflected in  $B$ , then in  $C$ , and will be recorded by a videocamera in  $D$ , provided that the viewing frustum of the videocamera is exactly aligned to the  $KC$  axis. The videocamera is mounted on the truss, while the rocker rotates about the  $KC$  axis together with the mirrors: however simple geometrical considerations show that the image recorded by the videocamera is always the same, that is a close-up picture of the revolute joint in  $A$ <sup>1</sup>.

---

<sup>1</sup>Except for the fact that the picture is rotated for a  $\beta$  angle on the viewing plane if the rocker rotates for a  $\beta$  angle

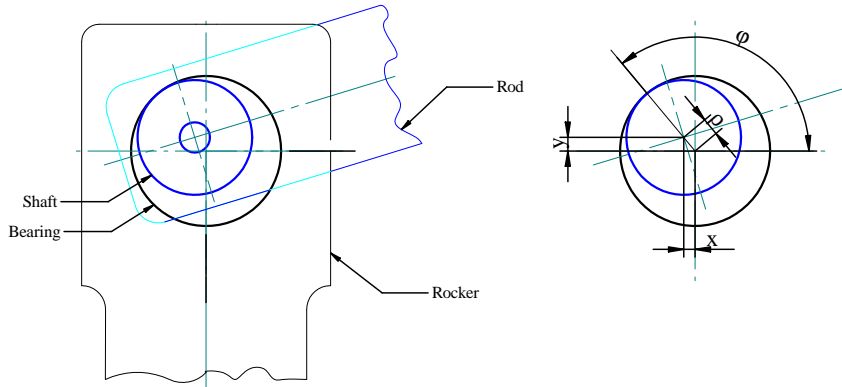


Figure 2: Scheme of the revolute joint with clearance and its reference coordinate systems (clearance is intentionally exaggerated for illustration purposes).

Of course the revolute joint in  $A$  is subject to strong accelerations because it follows an arched trajectory many times a second, so the upper mirror must be stiffly connected to the rocker in order to avoid oscillations of the mirror because of flexibility and inertial effects. To this end, we built a sturdy metallic structure which supports a lightweight mirror. Nonetheless, at very high rotation speeds, the structure bends a bit, but we tolerate this side effect because a stiffer fixture would have increased too much the mass of the device, hence affecting also the dynamics of the mechanism.

The lower mirror just rotates about  $KC$ , so it is subject to much lower inertial effects. It is mounted on a simple support made of plastic and metal.

The camera is mounted in  $D$  thanks to an adjustable tripod. Even small errors in positioning the camera (or in mounting the mirrors as depicted in Fig.3) will cause errors of two types: either the center of the bushing is not constantly visible at the same precise position into the recorded screen, either there is some kind of perspective distortion. Both kinds of error are inevitable, but they are corrected by our automatic image analysis software.

Looking at the scheme of Fig.3, it is possible to see that the viewing angle  $\alpha$  depends on the size of the joint to be recorded in  $A$ , and on the distance  $d = \overline{AB} + \overline{BC} + \overline{CD} + \overline{DE}$ . As a guideline, given  $r$  as the radius of the bushing to be recorded, we have:

$$\alpha = 2 \tan^{-1} \left( \frac{r}{d} \right).$$

Since in our setup we have approximately  $d = 1.5m$  and  $r = 20mm$ , it follows that telephoto lenses are needed. Moreover, it is advisable to keep  $d$  high (despite this implies a low  $\alpha$  angle and extreme telephoto lenses) because the lower  $\alpha$  is, the less is the perspective distortion.

Note that the distance  $\overline{AB}$  does not affect the optical behavior of the device; however a tradeoff must be found between the two opposite requisites of keeping the structure as stiff as possible (hence suggesting a low  $\overline{AB}$  offset) and allowing the illuminating light to reach the recorded joint without too many obstacles (thus suggesting a larger offset).

Illumination comes from a 1000W halogen lamp placed at the bottom of the mechanism. Ideally, also the light could follow a mirror maze as for the recorded images, but this is not practical for many reasons, so we preferred to directly illuminate the joint from below. Environmental lighting would be insufficient: the 1000W illumination is mandatory because the videocamera requires extreme lighting conditions when working at high speeds (1000 frames per second).

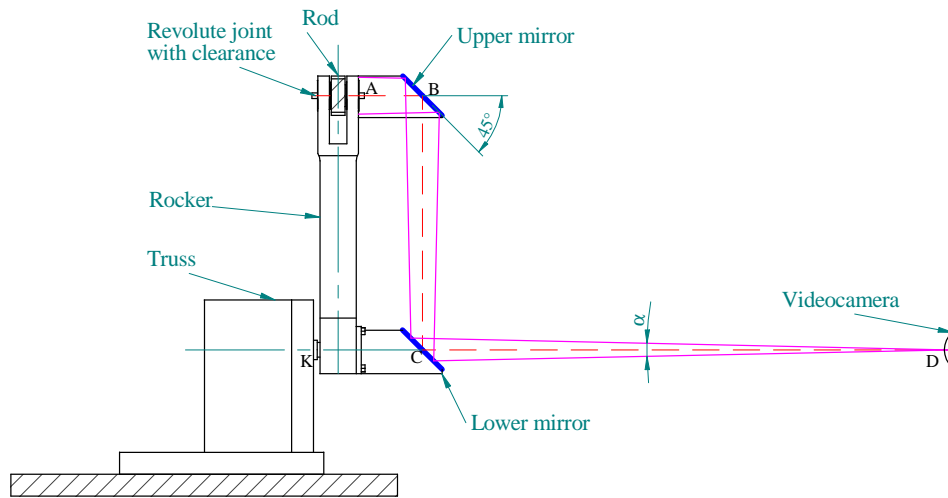


Figure 3: Mounting of the two mirrors on the oscillating rocker. Note the proper alignment of the videocamera and the reflections of the viewing frustum.

The videocamera, a DALSA CA-D6-0256W equipped with RAPITRON F1.8 14-75 mm zoom lenses, is capable of full-speed acquisition up to 1000 frames per second. The maximum resolution is 256x256 pixels, with direct hard disk streaming into uncompressed BMP images, using a custom parallel link to an on-board framebuffer. Image depth is 8-bit (256 shades of gray), giving a sustained bandwidth of 67Mb/s.

### 3 TESTS

Experimental tests have been performed with variable speed of the crank (160 rpm, 200 rpm, 300 rpm, 400 rpm, 500 rpm) and with different values of the clearance (from 0.1 mm up to 1 mm).

All tests have been recorded with the highest speed of the camera, that is 1000 fps (frames per second). Given some limitations on the throughput of the digital system, the maximum length of the acquired video is 1 second in all cases, which is enough to record at least two complete periods in the 160 rpm case.

The upper limit on the crank speed (500 rpm) is motivated by the fact that, for higher revolution speeds, there would be less than 100 frame samples per cycle at 1000 fps: this might be insufficient to capture high frequency oscillatory phenomena with sufficient details.

All video recordings have been saved as streams of uncompressed BMP images. Later, BMP streams have been converted in AVI animations with lossy compression (DivX encoding) for easy previewing.

### 4 AUTOMATIC IMAGE ANALYSIS

We developed a custom software for the automated image analysis of the video streams. This software operates on thousands of images, one by one, to recover the value of the  $\varphi$  angle of Figure 2, that is the position of the contact point as a function of time.

The automatic image analysis is complicated by many issues, most noticeably by the fact that illumination is not constant. In fact the lamp is mounted on a steady fixture while the joint moves on an arched trajectory, thus shadows are cast in variable directions. Also, most parts are made of

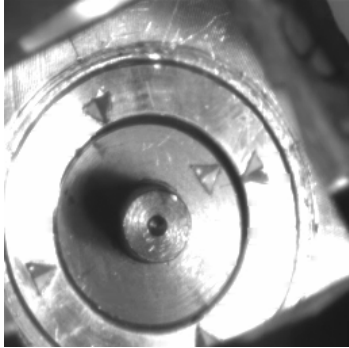


Figure 4: Step 1: the original picture, from the video stream acquired by the high-speed videocamera.

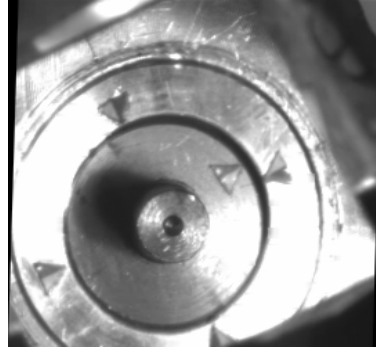


Figure 5: Step 2: linear affine transformation of the image, to correct shear and stretching caused by imprecisions in the alignment of mirrors and/or videocamera.

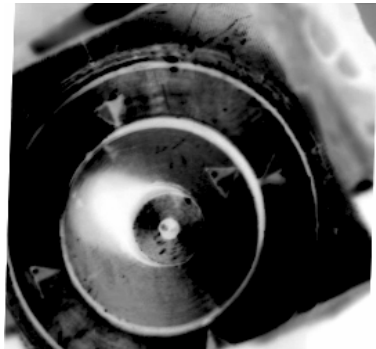


Figure 6: Step 3: histogram equalization, calibration of grayscale curve, and negative version of the image.

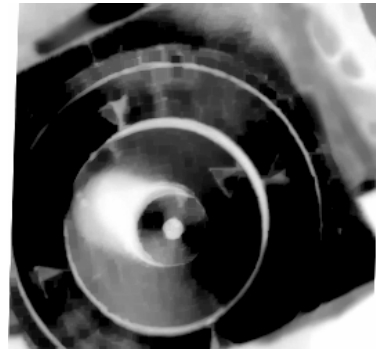


Figure 7: Step 4: morphological operator (dilation and erosion) to put in evidence the marker dot at the center.

polished metals, so there may be sudden flares and overlighting in some areas, for some positions of the rocker.

The program has been developed with the Matlab language, exploiting the features of the Image Processing Toolbox. In the following, we will describe the most relevant steps performed by the software, on a single image.

- Figure 4: the picture is loaded from disk and converted from 8-bit greyscale into a floating-point 64-bit grayscale representation, to avoid numerical entropy caused by the low dynamic range of the 8-bit format.
- Figure 5: a geometrical modification is performed on the entire picture, to correct errors caused by small misalignments of mirrors and/or camera. Otherwise, the bearing might look elliptic. The transformation is a linear affine mapping, which recovers shear and stretching distortions by applying a matrix transformation on the coordinates of the pixels. The matrix of the transformation, not necessarily orthogonal, has been computed by iterating adjustments by hand.
- Figure 6: we performed an histogram equalization of the image, so that the light values cover



Figure 8: Step 5: Reduction to single bitplane, with BW threshold, for edge detection.

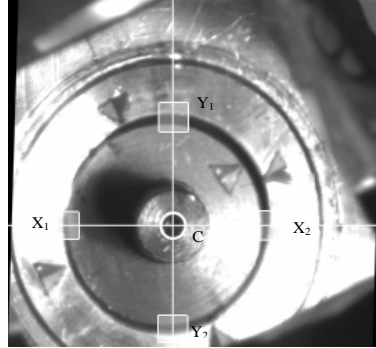


Figure 9: Step 6: Recognition of the center marker and cropping of four areas.



Figure 10: Step 7: Local corrections of highlighted areas to reduce the bloom effect, followed by elliptical masking, gamma correction and contrast enhancement.

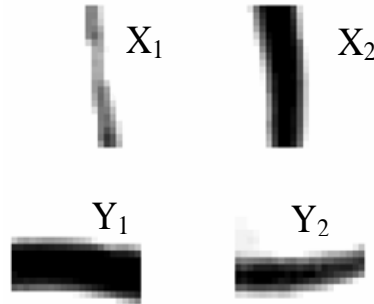


Figure 11: Step 8: Analysis of the clearance width in the four cropped areas, with averaging of results, for estimating the phase of the point of contact.

the entire visible range, without overall overlighting or underlighting. This is useful also because the lighting conditions change during the motion of the rocker. Also, we adjusted the contrast and the brightness, to put in evidence the useful details. Finally, we converted the image in negative grayscale.

- Figure 7: we applied a morphological operator on the image, to filter out unnecessary details and noise. We used the *image closure* morphological operator, which is equivalent to successive *dilation* and *erosion* operations, adopting a circular structuring element with radius  $r_s = 4$  pixels. This process is able to emphasize the small circular disc at the center of the shaft, which will be used to compute the coordinates of the center of the revolute joint. Note that inside that disc there was a small glossy highlight acting as a disturbance, but it is filtered away thank to the morphological operator.
- Figure 8: we convert the filtered image into a binary black and white mask, using an appropriate threshold. The mask will be used to find the edges of the binary areas (often called *blobs*). Edges are computed as arrays of x-y coordinates for polylines which border the white areas. After edge computations, we keep only the edge of the small dot at the center, which

can be recognized using some tests on the surface metrics: first of all, its area should fall between some min-max values, then its ratio area/perimeter should be about the same which can be seen in perfect discs, and finally the area should be as near as possible to the center of the image. With these conditions, it is possible to discard other white blobs which are not interesting.

- Figure 9: given that in the previous step we found the blob which represents the center of the shaft, it is also possible to compute its center using sub-pixel accuracy. This will be the center of the revolute shaft. Given the coordinates of the center, we extracted four areas  $X_1$ ,  $X_2$ ,  $Y_1$  and  $Y_2$ , where the gaps between the shaft and the bushing will be analyzed. Even if two areas, in quadrature, would be sufficient for the purpose of computing the displacement, we used four areas to improve accuracy and to minimize errors caused by image noise.
- Figure 10: a critical issue for analyzing the clearance is the fact that some parts of the image might be overlighted, while other might be too dimmed. For this reason, we applied different contrast and brightness corrections to different zones of a single image. In extreme situations, some areas reflect the light so hard that there are *bloom* and flare effects, therefore the width of the black arc (representing the clearance) could look smaller because of the light bleeding. The local grayscale adjustments can reduce these lighting artifacts, but not eliminate them completely. Note that in this step we also mask out the central part of the shaft and the outer part of the image using elliptical binary masks, since we already know the coordinates of the center of the clearance.
- Figure 11: the width of the four areas  $X_1$ ,  $X_2$ ,  $Y_1$  and  $Y_2$ , after contrast correction, are finally analyzed. Because of lighting artifacts, we cannot expect that the width of the black arcs can represent exactly the width of the underlying gap between shaft and bushing, but after some non-linear calibration we can get a reasonable information on the position of the point of contact.

All the steps above are repeated for all the pictures within a single video sequence, and the phase of the contact point  $\varphi$  can be plotted as a function of time.

Note that in some circumstances it is not possible to run through all the steps above successfully, either because the image is affected by too much noise, or because the illumination is deteriorated: in this case, we skip such an image. Later, skipped images are simply interpolated with adjacent frames.

## 5 CONCLUSIONS

Aiming at performing high-speed videocamera films of revolute pairs affected by clearance, we built a simple yet effective device based on the periscope concept. This system allows the close-up recording of oscillatory phenomena in the clearance even if the camera is fixed on the truss and the joint is moving along an arched trajectory with strong accelerations.

Also, we developed a software which can automatically process the video streams and find the motion of the shaft inside the bushing.

This experimental device, along with the custom image processing software, will be used to validate our numerical method for the simulation of clearances in articulated mechanism.

## 6 Acknowledgements

We thank Stefano Benacci for helping with the tests. We also thank Andrea Rossi and Carlo Dall'Asta for building and assembling the parts.

## References

- [A. Tasora, 2003] A. Tasora, E. Prati, M. S. (2003). Implementazione di un modello per contatto intermittente nelle coppie rotoidali con gioco. In *Proceedings of AIMETA '03, XVI Congresso Aimeta di Meccanica Teorica e Applicata*, Ferrara, Italy.
- [A. Tasora, 2004] A. Tasora, E. Prati, M. S. (2004). Experimental investigation of clearance effects in a revolute joint. In *Proceedings of AITC - Aimeta Tribology Conference*, Roma, Italy.
- [A. Tasora, 2005] A. Tasora, E. Prati, M. S. (2005). Un modello numerico per la previsione degli effetti dell'usura in coppie rotoidali con gioco. In *Proceedings of AIMETA '05, XVII Congresso Aimeta di Meccanica Teorica e Applicata*, Firenze, Italy.
- [A. Tasora, 2006] A. Tasora, E. Prati, M. S. (2006). A compliant measuring system for revolute joints with clearance. In *Proceedings of AITC-AIT International Conference on Tribology*, Parma, Italy.
- [P. Flores, 2006] P. Flores, J. Ambrosio, e. a. (2006). A study on dynamics of mechanical systems including joints with clearance and lubrication. *Mechanism and Machine Theory*, 41:247-261.
- [P. Flores, 2004] P. Flores, J. A. (2004). Revolute joints with clearance in multibody systems. *Computers & Structures*, 82:1359-1369.